Eur. Phys. J. E **2**, 343–350 (2000)

THE EUROPEAN PHYSICAL JOURNAL E

EDP Sciences

Shear-thickening transition in surfactant solutions: New experimental features from rheology and flow birefringence

J.-F. Berret[1,a], R. Gamez-Corrales[1], S. Lerouge[2], and J.-P. Decruppe[2]

[1] Unité Mixte de Recherche CNRS/Université de Montpellier II n° 5581, Groupe de Dynamique des Phases Condensées, F-34095 Montpellier Cedex 05, France
[2] Groupe de Rhéophysique des Colloides, Université de Metz, 57078 Metz - France

Received 11 November 1999

Abstract. We report on the shear-thickening transition observed in dilute aqueous solutions of cetyltrimethylammonium tosylate (CTAT) at concentrations $\phi \sim 0.2\%$. We have re-examined the kinetics of the shear-thickening transition using start-up experiments at rates above the critical shear rate $\dot{\gamma}_c$. Using simple well-defined protocols, we have found that the transient mechanical response depends dramatically on the thermal and on the shear histories. Using the same protocols, flow birefringence experiments were carried out. The gap of a Couette cell containing the sheared solution has been visualized between crossed polarizers in steady shear conditions, as well as in start-up experiments. We show that the birefringent shear-induced phase starts from the inner cylinder and grows along the velocity gradient direction, as in a shear banding situation. However, around $\dot{\gamma}_c$ we have not observed a regime of phase coexistence (isotropic and birefringent).

PACS. 83.50.By Transient deformation and flow; time-dependent properties: start-up, stress relaxation, creep, recovery, etc. – 83.50.Qm Thixotropy; thickening flows – 83.85.Ei Optical methods; sonography

1 Introduction

Among the rich variety of shear-induced instabilities and transitions encountered in surfactant systems, one of the most puzzling is the shear thickening effect observed in dilute or highly dilute solutions. It is now established that a prerequisite for the shear thickening is that the amphiphile molecules self-assemble in the quiescent state into locally cylindrical micelles. The shear thickening has been observed in solutions of rodlike aggregates in the dilute regime (case i) [1–7] but also in solutions of wormlike micelles in the entangled regime (case ii) [4,5,8–13]. Interestingly, some characteristic features of the transition are similar for rodlike and wormlike assemblies.

Dilute surfactant solutions have a zero-shear viscosity very close to that of the suspending solvent (~ 1 mPas) and no apparent viscoelasticity is observed. Under steady shear however, above a critical strain rate noted $\dot{\gamma}_c$ the shear viscosity increases, as a new and more viscous phase develops in the cell. The shear-induced phase (SIP) has been thoroughly investigated by rheological measurements [1–8,11], flow-birefringence [3,5,14] and small-angle neutron scattering [2–4,6]. The two latter techniques revealed a strong degree of alignment of this new phase with respect to the flow velocity. The microstructure and the mechanisms of formation of the shear-induced phase are not still understood.

One of the most remarkable properties is the kinetics of the transition. Starting from the quiescent state, when a solution is sheared at $\dot{\gamma} > \dot{\gamma}_c$, an induction time t_I is necessary to induce the viscous state. It has been reported by several authors [1,3,5,6,15] that t_I increases considerably when the applied shear rate approaches $\dot{\gamma}_c$ (keeping $\dot{\gamma} > \dot{\gamma}_c$). A dependence of the form $t_I \sim \dot{\gamma}^{-1}$ has been proposed [1,9]. On the other hand, when the shear is stopped, the initiated structure vanishes and it is usually assumed that the solution relaxes to its original state.

Here, we report on the binary surfactant system cetyltrimethylammonium tosylate/water (CTAT) at concentrations around $\phi \sim 0.2\%$, which correspond to the dilute regime (case i above). We have been urged to re-examine the kinetics of the shear-thickening transition for two reasons. First, the transient behaviors described above agree only qualitatively with what we have measured in CTAT systems. Second, even if great care is taken in the handling of the sample, nonreproducible transient measurements are obtained in the thickening regime. The kinetics is re-examined by shear rheology using simple protocols, and the transient mechanical response is found to depend dramatically on the thermal and on the shear histories. Using the same protocols, flow birefringence experiments were carried out and the gap of the shearing cell has been

[a] e-mail: berret@gdpc.univ-montp2.fr

visualized under crossed polarizers. We show that the birefringent shear-induced phase starts from the inner (rotating) cylinder and grows along the velocity gradient direction (as in shear banding [16–18]).

2 Experimental details

The cetyltrimethylammonium tosylate (CTAT) was purchased from SIGMA products (purity 99%) and used without further purification. The surface tension showed no minimum prior to the critical micelle concentration (CMC = 0.011 wt%), indicating that no surface active impurities are present in the CTAT. For rheological measurements, the samples were prepared with water that was purified by passing a Millipore water system. After their preparation, the solutions were stored several days at constant temperature ($T = 30\,^{\circ}$C) for equilibration. In order to avoid uncontrolled shear history, the solutions were gently poured into the shearing cells and were replaced just after in their storage chamber. All rheological measurements were made using a Rheometrics fluid spectrometer (RFS II) equipped with a Couette configuration with controlled shear rate (outer diameter 34 mm, gap 1 mm, the outer geometry rotates). Flow birefringence was carried out using an optical device described in detail in [19]. As for rheometry, the shearing cell is a Couette configuration (height 30 mm, gap 1 mm). Here the inner cylinder is 48 mm in diameter and rotates.

Mechanical and flow birefringence measurements were performed on two CTAT/H_2O solutions at $\phi = 0.16\%$ and $\phi = 0.24\%$. These concentrations were chosen since according to the recent literature [6,7,20,21], they are above the second critical micellar concentration ($\sim 0.04\%$) at which cylindrical micelles start to form, and below the overlap concentration ϕ^* which is the onset of semidilut regime. For CTAT at ambient temperature, the overlap concentration was estimated around $\phi^* \sim 0.7\%$ using transient electric birefringence [20] and fluorescence recovery [21], whereas viscosity measurements suggest a slightly lower value at $\phi^* \sim 0.5\%$. Both determinations are nevertheless in agreement. From electric birefringence, as well as from small-angle neutron scattering measurements, CTAT aqueous solutions at $\phi = 0.2\%$ are suspensions of short anisotropic aggregates of average length 200–300 Å(aspect ratio 4–6). The intermicellar distance was evaluated from the position of the first maximum of the structure factor, and was found to be around 600 Å [7].

3 Results

3.1 Shear rheology

Figure 1 shows the characteristic flow curve for CTAT at $\phi = 0.24\%$ and $T = 25\,^{\circ}$C. The stationary shear viscosity (filled circles) exhibits a clear Newtonian behavior for $\dot{\gamma} < 30\,\mathrm{s}^{-1}$ at a level that compares well to the viscosity of the solvent, $\eta_0 = 1 \pm 0.1$ mPas. Above a critical shear rate $\dot{\gamma}_c = 40 \pm 5\,\mathrm{s}^{-1}$ the viscosity increases,

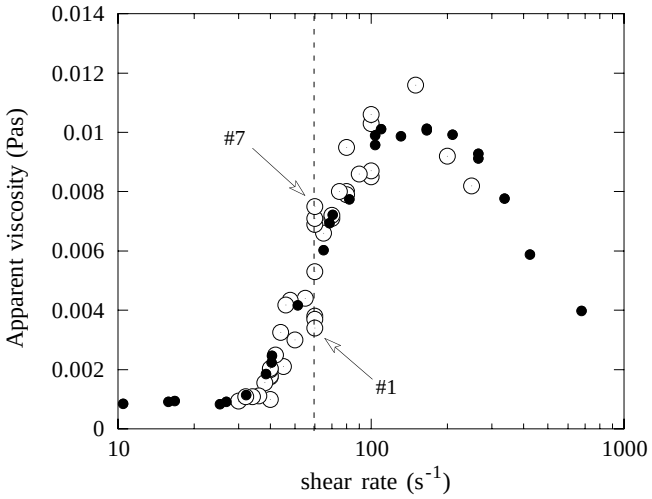

Fig. 1. Characteristic flow curves for CTAT aqueous solutions at $\phi = 0.24\%$ ($T = 25\,^{\circ}$C). The critical shear rate $\dot{\gamma}_c = 40 \pm 5\,\mathrm{s}^{-1}$ is defined by the onset of shear-thickening. Here, the stationary shear viscosity (filled circles) is compared to results obtained during a 4-hour run (empty circles) performed using start-up and step-down experiments at different shear rates between 5 and $500\,\mathrm{s}^{-1}$. The labels #1 and #7 refer to the first and seventh experiments carried out at $\dot{\gamma} = 60\,\mathrm{s}^{-1}$. The discrepancy between the two set of data is discussed in the text.

passes through a maximum ($\dot{\gamma} \sim 200\,\mathrm{s}^{-1}$) and then the solution shearthins. In Figure 1 we also show the results obtained during a 4-hour run at different shear rates between 5 and $500\,\mathrm{s}^{-1}$ (empty circles). During this run, the shear stress was recorded over time using start-up and step-down experiments. Above $\dot{\gamma}_c$, the data points scatter anomalously. For instance, seven tests were performed at $\dot{\gamma} = 60\,\mathrm{s}^{-1}$, and very surprisingly different stationary values of the viscosity were obtained. The term "stationary" refers here to a state characterized by a stress which is time independent over a period of, say 1000 s. At this rate, the induction time was $t_I = 180 \pm 30$ s (in contrast to, *e.g.*, [15], we define the induction time as the time needed for the measured shear stress to reach a stationary value). The first measurement at $\dot{\gamma} = 60\,\mathrm{s}^{-1}$ was performed after sample loading. It yields $\eta(\dot{\gamma} = 60\,\mathrm{s}^{-1}) = 3.4$ mPas (labeled #1 in Fig. 1) whereas the seventh and last measurement at $\dot{\gamma} = 60\,\mathrm{s}^{-1}$ gives $\eta = 7.4$ mPas (indicated by #7 in Fig. 1). Such a difference is far above the amplitudes of the oscillations usually shown by the transient viscosities in the thickened regime. On the contrary it suggests in these systems the existence of extremely long transients of the order of several hours.

In order to check the hypothesis of extremely long transient, we have repeated one given experiment several times. This experiment consists in applying a constant shear rate $\dot{\gamma} = 60\,\mathrm{s}^{-1}$ ($T = 25\,^{\circ}$C) to a freshly loaded CTAT solution at $\phi = 0.24\%$. The sample was delicately poured into the cell in order to avoid preshearing effects. Each sample was subjected to steady shear over a time period of $\sim 10^4$ s, and then a new sample was investigated.

Figures 2 show two examples of time responses collected over several hours. In Figure 2a, after the induction time of $t_I \sim 200\,s$ (inset), the apparent viscosity jumps up to 4 times the water viscosity and then a very slow increase is observed over the next 10^4 s. From 9×10^3 to 1.4×10^4 s, the viscosity has stabilized at $\eta_{ST} = 7.5\,mPas$. In another run, the induction time is again 200 s, but here $\eta(t)$ reached a much higher initial value, 10 mPs before slowly decreasing again to the stationary state at $\eta_{ST} = 7.5\,mPas$. After 3000 s, the shearing was stopped and the sample let free to relax in the quiescent state. The shearing was then resumed at the same shear rate and after t_I, the viscosity stabilizes rapidly to its former value. These two figures are in qualitative agreement with the data described in Figure 1. The time necessary to reach the steady state of shearing is much longer than the induction time, and apparently seems to depend on the history of the sample.

A second series of experiments was carried out, actually very similar to the previous one, but changing only the thermal history. The thermal treatment was applied prior any measurement. It consists in storing the solution in a high temperature chamber during 2 hours ($T = 90\,°C$). The hot liquid was then poured into the cell as explained previously and shearing is started only when the temperature was again stabilized at $T = 25\,°C$. Two examples of the time responses are displayed in Figure 3. In Figure 3a and Figure 3b, after inception of the shear, the viscosity remains at the solvent level over 2000 s! The induction time has now been multiplied by a factor 10. Then there is a first jump of the viscosity, to a rather low value (3-4 mPas) and then in Figure 3a a second step toward a regime of slowly increasing viscosity. If the shearing is stopped, and resumed in the same conditions as explained for Figure 2b, then the viscosity recovers its former value after the induction time of nearly 200 s. Finally, the ultimate value of the viscosity ($t > 10^4$ s) is found to be independent of the shear and thermal histories ($\eta_{ST} = 7 \pm 1\,mPas$), in agreement with the stationary data of Figure 1.

The stress signal during the induction period displays interesting features. Figure 4 is a zoom of transient viscosity data of Figure 3a about 1000 s before the onset of thickening (visualized by a rectangle in Fig. 3a). The shear viscosity exhibits four well-defined pretransitional oscillations of increasing amplitudes and period 150 s. At the end of this process, the system undergoes the thickening transition and at the scale of the oscillations the viscosity seems to diverge. However, several oscillations are not the rule. For most tests performed at $\dot\gamma = 60\,s^{-1}$, one small bump is usually observed before the system shear-thickens (as in Figs. 2a, 2b and 3b, see next section).

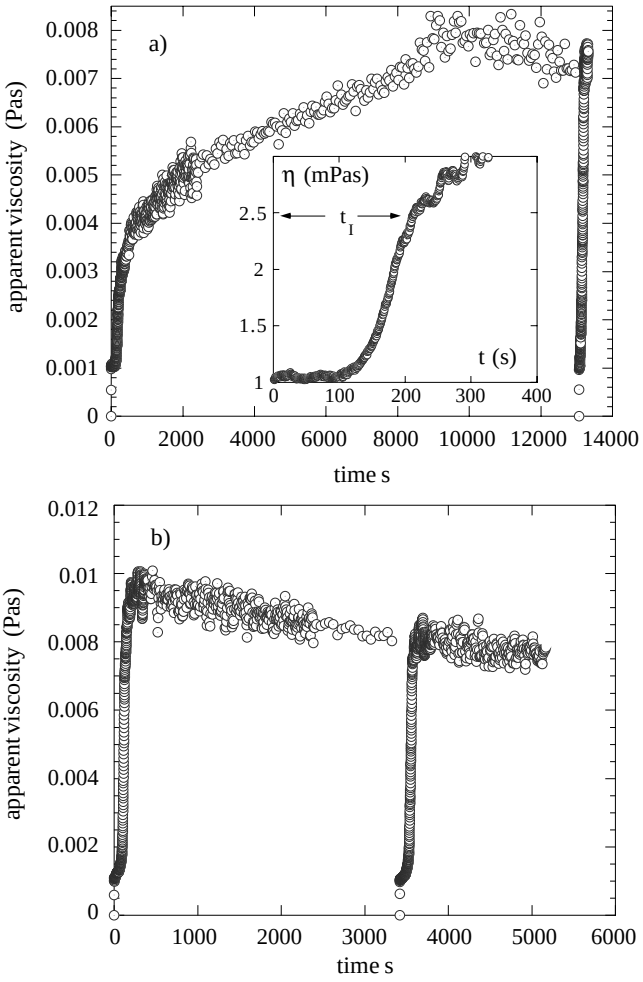

Fig. 2. Examples of transient shear viscosity obtained in start-up experiment at $\dot\gamma = 60\,s^{-1}$ for two samples that were handled similarly, from their preparation to their investigation. No heat treatment was applied. At $t \sim 12000$ s in a) and $t \sim 3000$ s in b), the shearing was stopped and the sample let free to relax in the quiescent state. The shearing was then resumed and the viscosity stabilizes within t_I to its former value. The inset is a zoom of a for times $t < 400$ s. It illustrates the initial kinetics and the induction time of ~ 180 s.

3.2 Flow-birefringence

The flow birefringence experiments were performed on a CTAT/H_2O solution at $\phi = 0.16\%$ and $T = 25\,°C$. Figure 5a shows the characteristic flow curve for this solution in stationary state. It strongly resembles that of Figure 1. The amplitude of the shear-thickening effect is different (5 against 10 mPas), but the critical shear rate comparable, $\dot\gamma_c = 40 \pm 5\,s^{-1}$. At this concentration, as for $\phi = 0.24\%$, extremely long transients were also observed, but they will not be discussed here. Figure 5b displays photographs of the 1 mm gap showing the light transmitted by the sheared fluid under crossed polarisers (at $\dot\gamma = 30, 40, 50, 80, 100$ and $200\,s^{-1}$, respectively). At $\dot\gamma = 40\,s^{-1}$ the solution is still isotropic and appears dark, whereas at $\dot\gamma = 50\,s^{-1}$ light is transmitted by the solution everywhere in the gap. This set of data shows that once the new phase is induced, it fills the gap of the shearing cell. As shown in Figure 5b, the increase of the viscosity coincides approximately with the development of the birefringent phase. A similar result was reported from small-angle neutron scattering experiments performed under shear on

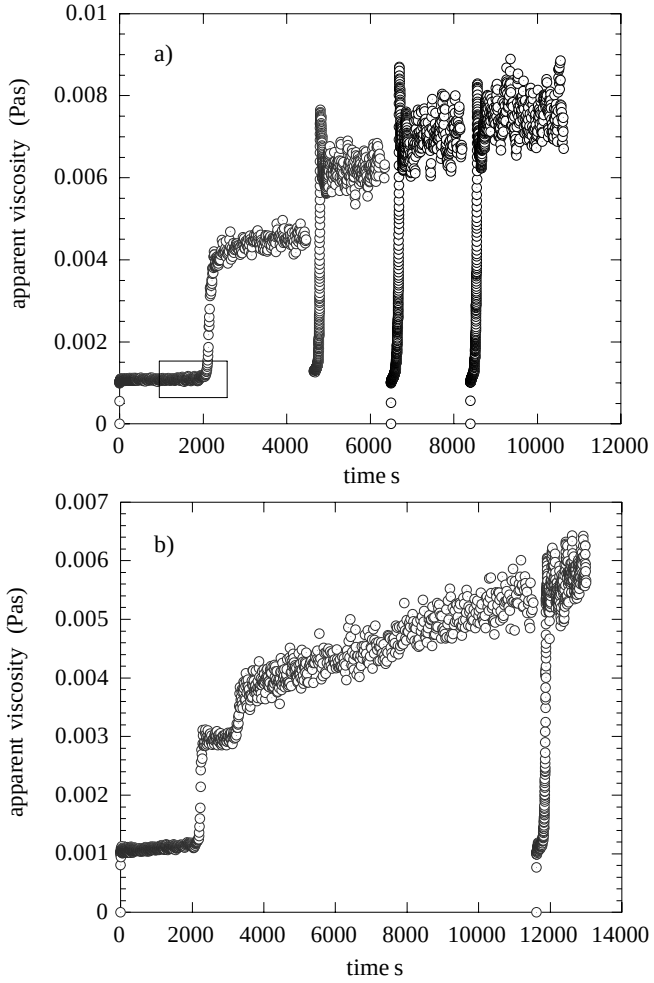

Fig. 3. Examples of transient shear viscosity obtained in start-up experiment at $\dot{\gamma} = 60\,\mathrm{s}^{-1}$ for two samples that were pre-heated at $T = 90\,^{\circ}\mathrm{C}$ for 2 hours. As in Figure 2, the shearing was stopped and resumed at the same shear rate several times.

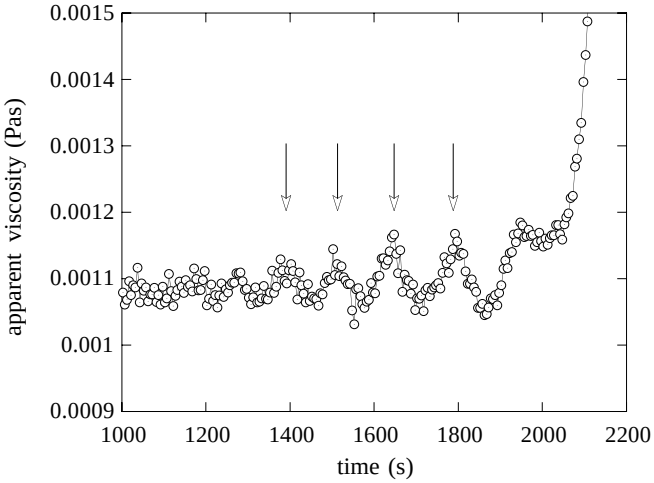

Fig. 4. Zoom of transient viscosity data of Figure 3a about 1000 s before the onset of thickening. The shear viscosity exhibits four well-defined pretransitional oscillations of increasing amplitudes and period 150 s. At the end of this process, the system undergoes the thickening transition.

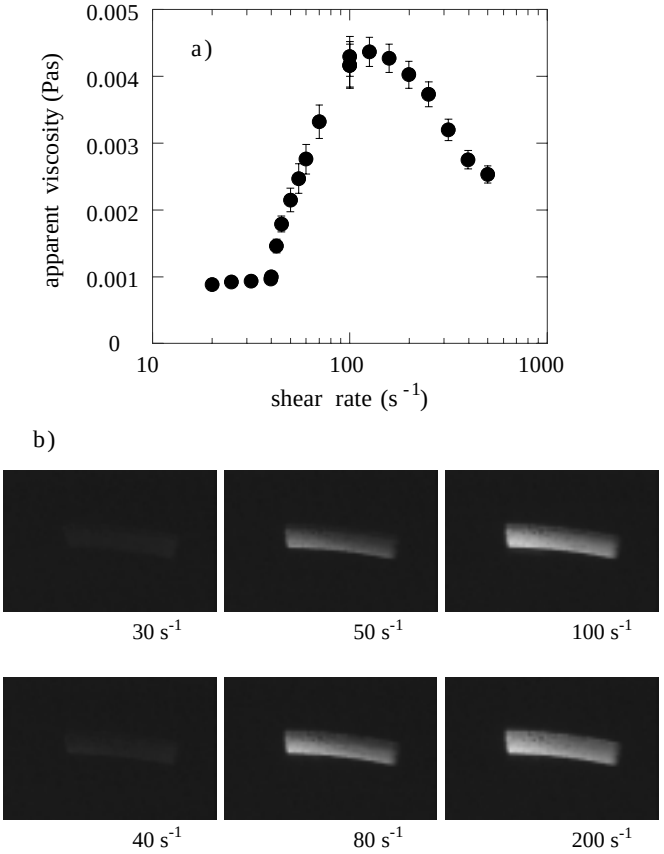

Fig. 5. a) Shear rate dependence of the stationary viscosity for a CTAT/H_2O solution at $\phi = 0.16\%$ ($T = 25\,^{\circ}\mathrm{C}$). b) Photographs of the 1 mm-gap showing the light transmitted by the sheared fluid under crossed polarisers at $\dot{\gamma} = 30, 40, 50, 80, 100$ and $200\,\mathrm{s}^{-1}$. The increase of the viscosity coincides approximately with the development of the birefringent phase. The two thin sub-bands close to the inner and outer cylinders (at $\dot{\gamma} = 50\,\mathrm{s}^{-1}$ and above) correspond to reflections of light on the walls of the cell (height 30 mm).

the same CTAT system [4,6]. More generally, this result corroborates the various flow birefringence measurements obtained on dilute systems these last years. As in references [3,14], we also found that the extinction angle χ of the SIP remains $\dot{\gamma}$-independent, at the value close to zero over the whole thickening and thinning ranges (for a review, see [3]). For $\dot{\gamma} > 40\,\mathrm{s}^{-1}$, we found $\chi_{\mathrm{ST}} = 0.7 \pm 0.3^{\circ}$. One advantage of the present technique is that it allows for the determination of the spatial distribution of the birefringence.

In this respect, Figure 5 deserves two additional comments. First, from the birefringence measurements alone, it seems that the solution undergoes an apparently abrupt transition from an isotropic to a birefringent state. Around $\dot{\gamma}_{\mathrm{c}}$ we have not observed a regime of phase coexistence between macroscopic layers (*e.g.*, isotropic/birefringent). Second, the intensity of the birefringence is not homogeneously distributed in the gap, it decreases with increasing radius. From the inner to the outer cylinder, Δn diminishes by nearly 40%, the extinction angle remaining at

the low value mentioned above (χ_{ST}). Note that the thin and bright bands close to the inner and outer cylinders (at $\dot{\gamma} = 50\,s^{-1}$ and above) are due to reflections of the transmitted light on the walls of the cell.

We now turn to the transient behavior of the birefringence in step-up experiments. Following the procedures derived in the rheology section, we have sheared the solution at high shear rate ($200\,s^{-1}$) over a long period, then reduced it to the value to be investigated ($100\,s^{-1}$). In order to ensure the reproducibility of the kinetics of growth of the SIP, we typically reproduced the late stage of Figure 3a (*i.e.* for $t > 8000\,s$), where the steady rotation of the cell is stopped and resumed repeatedly. Figure 6 shows the sequence of photographs taken during one of these step-shear rate experiments at $\dot{\gamma} = 100\,s^{-1}$. Three time regimes can be distinguished.

Regime 1: Up to 10 s after the inception of shear, no birefringence can be detected.

Regime 2: Around $t \sim 12\,s$ the birefringence shows up at the vicinity of the inner cylinder. Then, the intensity increases noticeably ($t > 14\,s$) and spreads out in the gap. At the end of the second time regime ($t \sim 28\,s$), the whole gap appears birefringent between crossed polarizers.

Regime 3: In the third regime, $t > 28\,s$, the birefringence increases continuously and reaches finally the steady state at $t \sim 36\,s$.

Figure 7 shows the mechanical response corresponding to the same experimental conditions as in Figure 6 (start-up experiment at $\dot{\gamma} = 100\,s^{-1}$). Several successive runs are shown that illustrate the reproducibility of the temporal dependence of viscosity increase. $\eta(t)$ remains constant during the first $\sim 10\,s$, exhibits a shoulder between 15 and 30 s and then increases by a factor 4 in the stationary state. Flow birefringence photographs representative of each time regime are included to the figure for comparison ($t = 14, 28$ and 50 s). In terms of the kinetics of the shear-thickening transition, it seems clear that the shoulder in the transient viscosity coincides rather accurately to the birth and growth of the SIP. A more surprising result is the shift between the times at which the stationary state of the viscosity (at around $t = 50\,s$) and that of the flow birefringence (end of *Regime* 3, $t \sim 36\,s$) are observed. It is possible that concerning this later result, geometry effects such as the curvature of the rotating cylinders are playing a role on the time scale of the kinetics (see discussion below).

4 Discussion

Figures 2–4 have demonstrated that the kinetics of the shear-thickening transition as followed by the mechanical response in start-up experiments is complex. Repeating the same experiment several times on a freshly loaded sample, we found reproducibly that the viscosity increases within an induction time $t_I \sim 180\,s$. However, the height of the viscosity jump clearly depends on the rheological history (if the solution was presheared or not), but more surprisingly it varies also from sample to sample. For the present data, the initial jump in $\eta(t)$ for solutions which were not preheated is comprised between 3.5 and 10 mPas. This first jump is then followed by a slow evolution of the mechanical response (increase or decrease, according to the height of the first step) toward a state that can be regarded as the stationary state of flow.

Preheated solutions exhibit longer induction times. For the two examples discussed in the experimental section, this time is around 2000 s. Actually, depending on the runs, induction times were found to vary between 1000 s and 3000 s for comparable heat treatments (say, 2 hours at 90 °C). The crucial result, however is that the induction time is by far much longer that the induction time for samples which were not preheated. For preheated solutions, the temporal variation of the shear viscosity usually exhibits an increase in two steps. Three steps or more have not been evidenced so far. After a shearing time of $\sim 10^4\,s$ (at $\dot{\gamma} = 60\,s^{-1}$), the stationary regime is reached and the reproducibility of start-up experiments is ensured. The previous experiments were performed at a shear rate which is about $20\,s^{-1}$ above $\dot{\gamma}_c(\dot{\gamma} = 60\,s^{-1}, \dot{\gamma}_c = 40 \pm 5\,s^{-1})$. If the difference $\dot{\gamma} - \dot{\gamma}_c$ is reduced, the overall kinetics of the shear-thickening transition is slower. On the contrary if this difference $\dot{\gamma} - \dot{\gamma}_c$ is made larger, reproducible steady states are easier to obtain.

The above results suggest that the state of aggregation in the quiescent solution and the kinetics of the thickening transition are interrelated. One possible explanation would be that the surfactant solutions are in a metastable self-assembling state, due for instance to the long-range electrostatic interactions [7]. This metastable state could then be described as a coexistence state of short rodlike aggregates [7] and slowly evolving supramolecular structures, such as huge micelles [22] or pieces of entangled network [5]. These structures would then depend on the thermal and rheological treatments and would act as nuclei for the shear-thickening transition .

Using flow birefringence, one noticeable result is the discontinuity of the transition seen in Figure 5b. The steady state measurements show that once the new phase is induced, it fills the gap of the shearing cell. This is a major point for at least two reasons. A discontinuity of the mechanical response at the shear-thickening transition has been recently reported on parent compounds [9]. Thus, the question to know if other physical quantities could be also discontinuous is still open. Second, the results of Figure 5b are in apparent contradiction with the rheology data of Figure 5a, which display a continuous increase of the viscosity. Actually, this contradiction can be solved from a closer analysis of the transients in Figures 6 and 7. The transition from an isotropic to a birefringent solution occurs in three steps (see previous section). The second step corresponds to the birth and growth of the SIP ($14\,s < t < 28\,s$) and seems to fit the shoulder in the transient viscosity quite well. Therefore, even if geometry effects are slightly modifying the time scale of the kinetics when passing from rheology to birefringence, we are allowed to conclude from Figure 7, that the sheared solution is becoming birefringent *before* the steep and

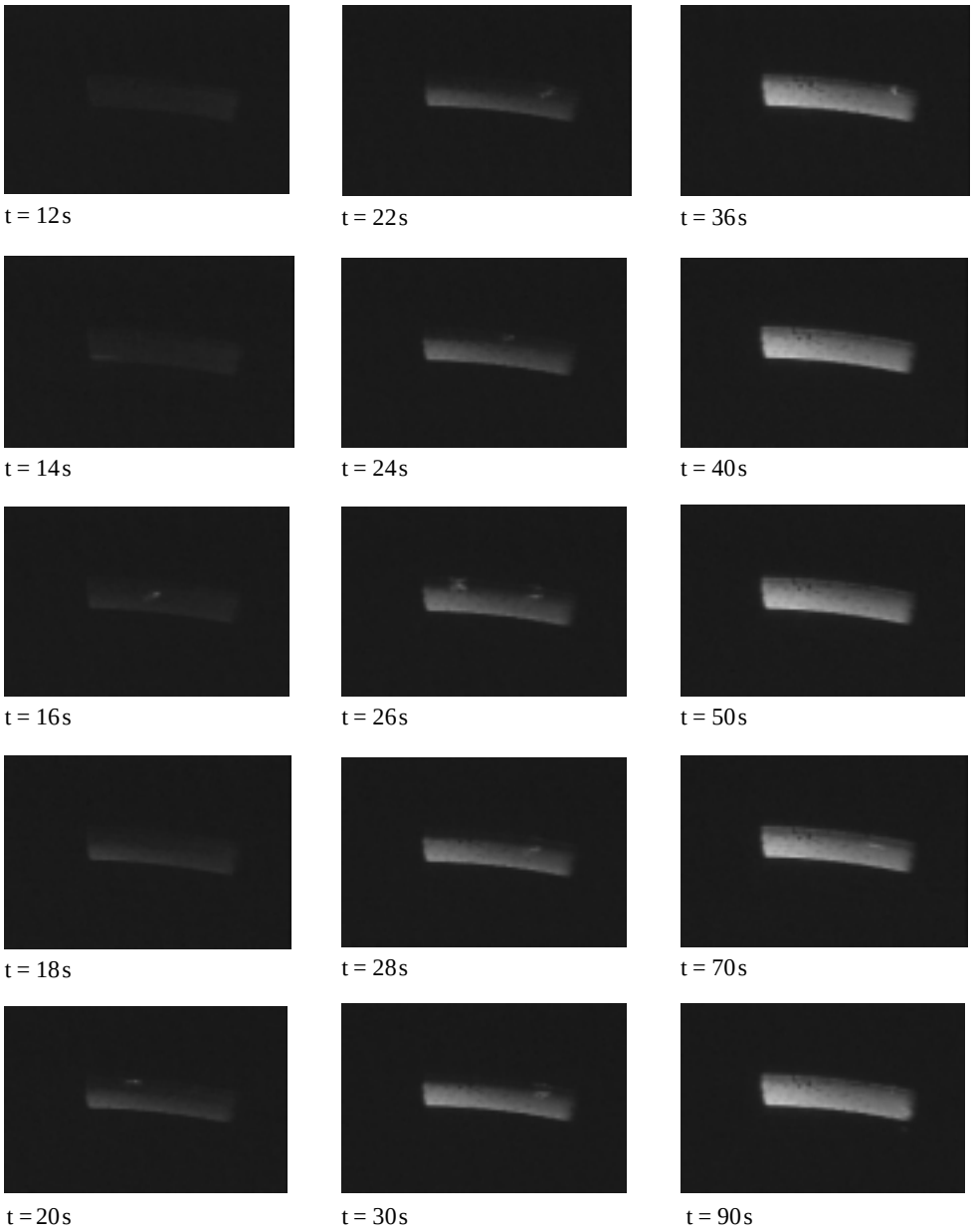

Fig. 6. Sequence of photographs taken during one step-shear rate experiment at $\dot{\gamma} = 100\,\mathrm{s}^{-1}$. 10 s after inception of the shear, no birefringence can be detected. Around $t \sim 12\,\mathrm{s}$ the birefringence shows up at the vicinity of the inner cylinder and filled the gap at $t \sim 28\,\mathrm{s}$. In the late stage, $t > 28\,\mathrm{s}$, the birefringence increases continuously and reaches the steady state ($t = 36\,\mathrm{s}$).

final increase of the viscosity. In other words, the surfactant solution can become birefringent and nevertheless the viscosity remains close to that of the solvent. At the so-called shoulder ($14\,\mathrm{s} < t < 28\,\mathrm{s}$), the apparent viscosity is not more than 1.5 time that of the solvent. According to us, this could explain why in steady state conditions the shear-thickening transition appears as continuous in rheology and discontinuous in flow birefringence.

Second, the shear-thickening transition bears some similarities with the shear-banding instability observed in semi-dilute and concentrated wormlike micelles [16–18]. As for shear-banding, the shear-induced phase grows from the inner cylinder to the outer one, *i.e.* along the velocity gradient direction. We have also checked that macroscopic phase separation does not occur in the vorticity direction. This is an important result since it has been suggested recently by several authors that underlying the shear thickening transition there might be a constitutive equation which is multivalued in stresses [23,24]. If this were the case, phase separation should occur at a given shear rate with the interface between bands perpendicular to the vorticity direction [10]. This arrangement can be visualized as disks of matter stacked from the bottom to the top of the Couette, and supporting different stresses. Obviously, in CTAT this is not the case.

For the configuration used in flow birefringence (inner radius 24 mm, gap 1 mm), there is an excess shear rate or shear stress of $\sim 8\%$ for the fluid close to the

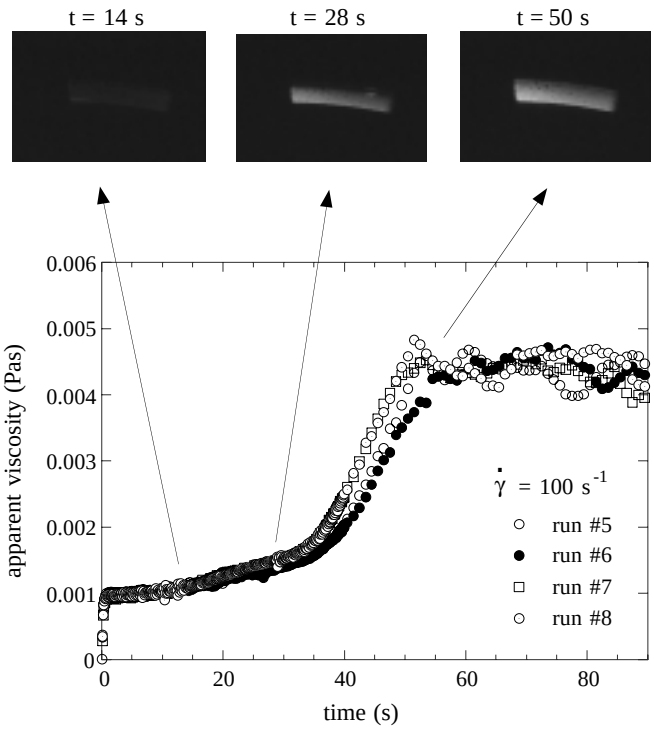

Fig. 7. Transient viscosity data corresponding to the same experimental conditions as in Figure 6 (star-up experiment at $\dot{\gamma} = 100\,\mathrm{s}^{-1}$). Several successive runs are shown to illustrate the reproducibility of the viscosity increase. Flow birefringence photographs representative of each time regime are included ($t = 14, 28$ and 50 s). From this comparison, we ascribe the shoulder in the viscosity data between 15 and 30 s to the birth and growth of the SIP.

inner cylinder, as compared to the outer one. And we have found in Figure 6 that the SIP shows up close to the inner cylinder, where the stress (and rate) is the largest. This is an indication that the inhomogeneity of the velocity field is important in determining the kinetics of the thickening transition, but also the critical shear rate and the viscosity jump [8,13]. There is however one major difference with the shear-banding instability. Here, for dilute surfactant solutions we found no evidence of coexisting phases under shear, as is the case at the stress plateau of wormlike micelles.

5 Concluding remarks

There is one essential new feature in the rheology of the shear-thickening transition. The mechanical response varies from test to test, for samples that have been treated exactly in the same way from their preparation to their investigation. To our knowledge this aspect has not been emphasized so far in dilute solutions. Somewhat similarly, but in more concentrated wormlike micelles, recent investigations by Britton and Callaghan [25] have demonstrated the strong sensitivity of shear-banding to impurities. In CTAT dilute solutions, the lack of reproducibility might indicate that these surfactant solutions are characterized by long-lived metastables states. This latter statement needs to be checked by other experimental techniques. Interesting phenomena in the time-dependent viscosity such as long transients, pretransitional oscillations, intermediate stable states, etc. have been also found out, but no explanation is provided here.

The flow birefringence results indicate that the shear-thickening transition coincides approximately with the development of a birefringent and highly aligned phase[2–4, 6,14]. However, the kinetics of the transition as deduced from the transients reveals a complex scenario, with several time regimes. Interestingly, the birth and growth of the SIP starting from the inner cylinder occurs prior to the viscosity increase. This suggests the existence of a delay (in time and/or shear rate) between the development of the SIP and the shear-thickening transition. Finally, we would like to emphasize that, although the viscosity increases above $\dot{\gamma}_c$, this shear-induced phase is characterized by an extinction angle χ close to zero, and that it remains so over the whole shear-thickening and shear-thinning ranges. This is a crucial result, already known from previous reports [3,14], but it indicates for the SIP a strong alignment of the micellar aggregates with respect to the flow.

We acknowledge Peter Olmsted and Heinz Hoffmann for fruitful discussions. We also thank the GDR 1081 "Rhéophysique des Colloïdes et Suspensions" of the CNRS for stimulating environment and for financial support.

References

1. H. Hoffmann, G. Platz, H. Rehage, W. Schorr, W. Ulbricht, Ber. Bunsenges. Phys. Chem. **85**, 255 (1981).
2. P. Lindner, H.W. Bewerdorff, R. Heen, P. Sittart, H. Thiel, J. Langowski, R. Oberthur, Progr. Colloid Polym. Sci. **81**, 107 (1990).
3. S. Hofmann, A. Rauscher, H. Hoffmann, Ber. Bunsenges. Phys. Chem. **95**, 153 (1991).
4. V. Schmitt, S. Schosseler, F. Lequeux, Europhys. Lett. **30**, 31 (1995).
5. R. Oda, P. Panizza, M. Schmutz, F. Lequeux, Langmuir **13**, 6407 (1997).
6. J.-F. Berret, R. Gamez-Corrales, J. Oberdisse, L.M. Walker, P. Lindner, Europhys. Lett. **41**, 677 (1998).
7. R. Gamez-Corrales, J.-F. Berret, L.M. Walker, J. Oberdisse, Langmuir **15**, 6755 (1999).
8. A.M. Wunderlich, P.O. Brunn, Colloid Polym. Sci. **267**, 627 (1989).
9. P. Boltenhagen, Y. Hu, E.F. Matthys, D.J. Pine, Phys. Rev. Lett. **79**, 2359 (1997).
10. E.K. Wheeler, P. Fischer, G.G. Fuller, J. Non-Newtonian Fluid Mech. **75**, 193 (1998).
11. V. Hartmann, R. Cressely, Europhys. Lett. **40**, 691 (1997).
12. H.T. Hu, P. Boltenhagen, D.J. Pine, J. Rheol. **42**, 1185 (1998).
13. Y.T. Hu, P. Boltenhagen, E. Matthys, D.J. Pine, J. Rheol. **42**, 1209 (1998).

14. I. Wunderlich, H. Hoffmann, H. Rehage, Rheol. Acta **26**, 532 (1987).
15. P. Boltenhagen, Y. Hu, E.F. Matthys, D.J. Pine, Europhys. Lett. **38**, 389 (1997).
16. R. Makhloufi, J.-P. Decruppe, A. Aït-Ali, R. Cressely, Europhys. Lett. **32**, 253 (1995).
17. R.W. Mair, P.T. Callaghan, J. Rheol. **41**, 901 (1997).
18. J.-F. Berret, G. Porte, J.-P. Decruppe, Phys. Rev. E **55**, 1 (1997).
19. J.-P. Decruppe, R. Hocquart, T. Wydro, R. Cressely, J. Phys. (France) **50**, 3371 (1989).
20. J. Narayanan, E. Mendes, C. Manohar, J. Phys. Chem. **100**, 18524 (1996).
21. J. Narayanan, W. Urbach, D. Langevin, C. Manohar, R. Zana, Phys. Rev. Lett. **81**, 228 (1998).
22. E.W. Kaler, K.L. Herrington, A.K. Murthy, J.A.N. Zasadzinski, J. Phys. Chem. **96**, 6698 (1992).
23. G. Porte, J.-F. Berret, J.L. Harden, J. Phys. II (France) **7**, 459 (1997).
24. P.D. Olmsted, Curr. Opin. Colloid Interface Sci. **4**, 95 (1999).
25. M.M. Britton, P.T. Callaghan, Eur. Phys. J. B **7**, 237 (1999).